Electronic Characterization of 1-Keto-4-thioketo-3,6-diphenylpyrrolo[3,4-*c*]pyrrole in Solution and in the Solid State

J. Mizuguchi

Department of Applied Physics, Faculty of Engineering, Yokohama National University, 79-5 Tokiwadai, Hodogaya-ku, 240-8501 Yokohama, Japan

Received: August 2, 2000

The title compound, 1-keto-4-thioketo-3,6-diphenypyrrolo-[3,4-*c*]-pyrrole (MTPP) is a mono-thionated derivative of diketopyrrolopyrrole (DPP) that is known as a novel red pigment on the market. Dithioketo-pyrrolopyrrole (DTPP) has also attracted attention as a material useful for laser printers as well as optical disks based on GaAsAl laser diodes. Because of the hybrid structure of DPP and DTPP, the electronic structure of MTPP has been characterized in solution and in the solid state in order to explore new electronic applications. The crystal structure of MTPP is found to be isomorphous with modification I of DTPP. The color of MTPP is nearly between DPP and DTPP. The intermolecular hydrogen bonds based on both NH···O and NH···S are found to be considerably weak as compared with those of DPP (NH···O) and DTPP (NH···S). The absorption spectrum of evaporated MTPP suggests a potential application for the blue-filter for liquid crystal displays (LCD).

1. Introduction

1,4-Diketo-3,6-diphenylpyrrolo[3,4-*c*]pyrrole (DPP; Figure 1) is a heterocyclic, red pigment based on a novel chromophore of diketopyrrolopyrrole.[1] DPP pigments have been on the market since 1986 and a series of investigations have been carried out on the crystal structure[2−5] and electronic properties,[6−11] including unconventional applications to electrochromic displays and others. On the other hand, dithioketopyrrolopyrrole (DTPP; Figure 1) has also attracted attention as a material suitable for laser printers[12−14] as well as optical disks[15,16] based on GaAsAl diode lasers. In DTPP, there are three crystal modifications,[17,18] among which only modification III exhibits an intense near-IR absorption. The electronic structure as well as the mechanism of the near-IR absorption are fully characterized by spectroscopic means and molecular orbital calculations.[19−21]

The title compound, 1-keto-4-thioketo-3,6-diphenylpyrrolo-[3,4-*c*]pyrrole, is a mono-thionated DPP (abbreviated to MTPP shown in Figure 1). Because of the hybrid structure between DPP and DTPP, the electronic structure of MTPP has been characterized in the present investigation in order to explore novel electronic applications.

2. Experimental Section

2.1. Single Crystals and Evaporated Films of MTPP. MTPP was prepared according to the procedure reported previously.[22] The single crystals of MTPP were grown from the vapor phase using a two-zone furnace.[23] The crystal structure was analyzed by a Rigaku X-ray diffractometer AFC7R.[24] The evaporated films of MTPP were prepared under high vacuum onto glass substrates for measurements of absorption spectra (thickness: ca. 1000 Å) and X-ray diffraction diagrams (ca. 3000 Å) and onto KBr disks for measurements of IR spectra (ca. 3000 Å). Vapor treatment of MTPP was carried out by exposing the evaporated films to acetone vapor for about 1 h in order to induce molecular rearrangement.

2.2. Measurements. The solution and solid-state spectra were measured on a Shimazu spectrophotometer (UV-2400PC).

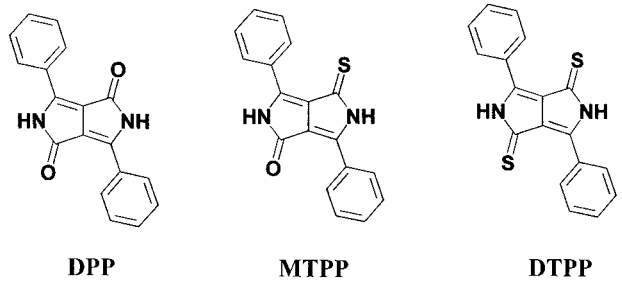

Figure 1. Molecular structures for DPP, MTPP, and DTPP.

Electrical conductivities in solution were measured with a TOA CM-2A conductometer. The temperature dependence of the absorption spectra of evaporated MTPP was measured in the range between 12 and 293 K on the above spectrophotometer in combination with a cryostat from Iwatani Gas Co. Ltd. (model: CRT-105-OP). Polarized reflection spectra were measured on single crystals of MTPP by means of a UMSP 80 microscope−spectrophotometer (Carl Zeiss) equipped with an R928 photomultiplier (HTV). An Epiplan Pol (×8) objective was used together with a Nicol-type polarizer. Reflectivities were corrected relative to the reflection standard of silicon carbide. Thermogravimetric analysis (TGA) was carried out under vacuum or in air on powdered DPP, MTPP, and DTPP using a Mettler thermoanalysis system TA 2000. TGA measurements were made with a heating rate of 4 K/min.

2.3. Molecular Orbital (MO) Calculations. Geometry of the MTPP molecule was optimized by the AM1 Hamiltonian of MOPAC93[25] for the initial state as well as mono-deprotonated and di-deprotonated states in the form of $>N^-$. The optical absorption bands were then computed on the optimized geometry using the PPP and CNDO/S Hamiltonians. The PPP calculations were carried out, using the variable β (resonance integral), γ (electron repulsion)-approximation. The standard parameters were taken from ref 26. The CNDO/S program used was a modified version of the CNDO/2 (QCPE#141) to include the configuration interaction.[27] The two basis sets, *sp* or *spd*,

10.1021/jp0027905 CCC: $20.00
Published on Web 01/27/2001

TABLE 1: Crystallographic Data for DPP, MTPP, and DTPP

			DTPP[17,18]		
	DPP[2]	MTPP[24]	modification I	modification II	modification III (near-IR abs.)
chemical formula	$C_{18}H_{12}N_2O_2$	$C_{18}H_{12}N_2OS$	$C_{18}H_{12}N_2S_2$	$C_{18}H_{12}N_2S_2$	$C_{18}H_{12}N_2S_2$
molecular symmetry	C_i	C_1	C_i	C_i	C_2
formula weight	288.31	304.37	320.43	320.43	320.43
Z	1	2	2	2	4
space group	$P-1$	$P2_1/n$	$P2_1/n$	$P2_1/n$	$C2/c$
a (Å)	3.817(1)	7.570(3)	7.986(1)	4.873(1)	27.008(4)
b (Å)	6.516(1)	4.869(3)	4.757(1)	18.613(2)	6.982(1)
c (Å)	13.531(2)	19.616(4)	19.685(3)	7.995(1)	7.935(1)
α (°)	93.11(1)				
β (°)	86.97(1)	99.07(3)	99.18(2)	95.76(2)	100.64(1)
γ (°)	95.02(1)				
V (Å^3)	334.3(2)	714.0(6)	738.2(5)	721.5(5)	1470.6(7)
molecular stack	pseudo bricks in a brick wall	herringbone	herringbone	herringbone	bricks in a brick wall

TABLE 2: Calculated Optical Absorption Bands for the Initial, Mono- and Di-deprotonated States of MTPP

			observed		PPP		CNDO/S	
charge	heat of formation (kJ/mol)	basis set	λ (nm)	log ϵ	λ (nm)	f	λ (nm)	f
0	53.4	*p*	580.0	4.20	531.7	0.775	430.0	0.713
(initial state)		*spd*					430.0	0.709
−1	288.9	*p*	620.0	4.20			493.8	0.377
(mono-deprotonated state)		*spd*					493.7	0.379
−2	470.1	*p*	662.5	4.18			533.2	0.489
(di-deprotonated state)		*spd*					532.8	0.489

are available. The Mataga−Nishimoto equation was used in the PPP and CNDO/S calculations for the evaluation of electronic repulsion integrals.[28] Sixty and 99 configurations were considered for the configuration interaction (CI) for the PPP, and CNDO/S calculations, respectively. All calculations were made on an RS6000 IBM workstation.

3. Results and Discussion

3.1. Crystal Structure.[24] Table 1 details the crystallographic data for MTPP together with DPP and DTPP (modifications I, II, and III). It is readily apparent that the present MTPP structure is isomorphous with modification I of DTPP.[17] The MTPP molecule is asymmetric and thus characterized by a dipole moment of about 1.1 *D* as calculated by MOPAC93.[25] The phenyl rings are twisted parallel out of the planar heterocyclic system by about 6.3(7)°. The oxygen and sulfur atoms are not entirely on the plane of the heterocyclic system, but are located slightly below and above the plane by about 0.17(1) and 0.09(1) Å, respectively.

Figure 2 shows the projection of the structure onto the (*a*,*c*) plane, in which the intermolecular hydrogen bonds are designated as dotted lines. The molecules are oriented in the same direction on the molecular plane and are stacked in a herringbone fashion along the *b*-axis. On each side of the molecule, two kinds of the hydrogen bonds are formed: one is based on NH···O and the other is NH···S. The angle of the NH/O and distances between O/H, N/H, and N/O are 156.45 °, 2.14, 0.95 and 3.04(1) Å, respectively; whereas those of NH/S and S/H, N/H and N/S are 154.70 °, 2.31, 0.95, and 3.21(1) Å, respectively. The N/O and N/S distances in MTPP are, respectively, lengthened and shortened as compared with those of DPP[2] (2.817(4) Å) and DTPP[17,18] (3.435(3), 3.440(5), and 3.359(5) Å for modifications I, II, and III, respectively).

3.2. Solution Spectra. Figure 3 shows the solution spectrum of MTPP in dimethyl sulfoxide (DMSO). Since the MO calculations shown in Table 2 reveals that there is only one single electronic transition in the visible region and, in addition, a series of absorption bands (Figure 3) are equally spaced of about 1400 cm^{-1}, the absorption band in the longest wavelength is ascribed to the pure electronic transition denoted by the 0−0 transition, followed by the 0−1, 0−2, 0−3, and 0−4 transitions. Deprotonation of MTPP by means of an alikali induces significant changes in absorption spectra as described below: $>NH + OH^- \rightarrow >N^- + H_2O$.

Figure 4 shows the specific conductivity of MTPP solution in DMSO plotted against the molar ratio of tetrabutylhydroxide (TBAH) to MTPP. The conductivity of the solution increases linearly from the start of the titration. This represents the neutralization of the weak acid (MTPP) and the replacement by its salt that is a strong electrolyte. Point A is the first end point corresponding to the mono-deprotonation. From point A, the conductivity increases with a higher gradient up to point B which corresponds to the di-deprotonation. The increase in conductivity after point B is attributed to the intrinsic conductivity of TBAH in DMSO.

The absorption spectra between the initial point and point A as well as those between points A and B are shown in Figures 5a and 5b, respectively. The absorption bands on deprotonation are qualitatively in good agreement with the MO-calculations shown in Table 2 for the initial, mono-deprotonated, and di-deprotonated states.

3.3. Solid-State Spectra of Evaporated MTPP and Their Temperature Dependence. Figure 6 shows the absorption spectra of evaporated MTPP before and after vapor treatment. The absorption bands as evaporated appear around 550 and 610 nm together with a shoulder at about 510 nm. Vapor treatment then brings about a small shoulder around 700 nm (not presented here) and it grows up finally to an intense band as shown in Figure 6, while the intensity of the two visible bands around 550 and 610 nm is greatly diminished.

It should be noted here that the optical absorption of MTPP is minimum around 420 nm and the visible bands cover the spectral region of green (555 nm) and red (620 nm) in both spectra before and after vapor treatment. Therefore, MTPP can be used as a blue filter with high purity for applications of liquid crystal displays (LCD). The spectral characteristic is equivalent

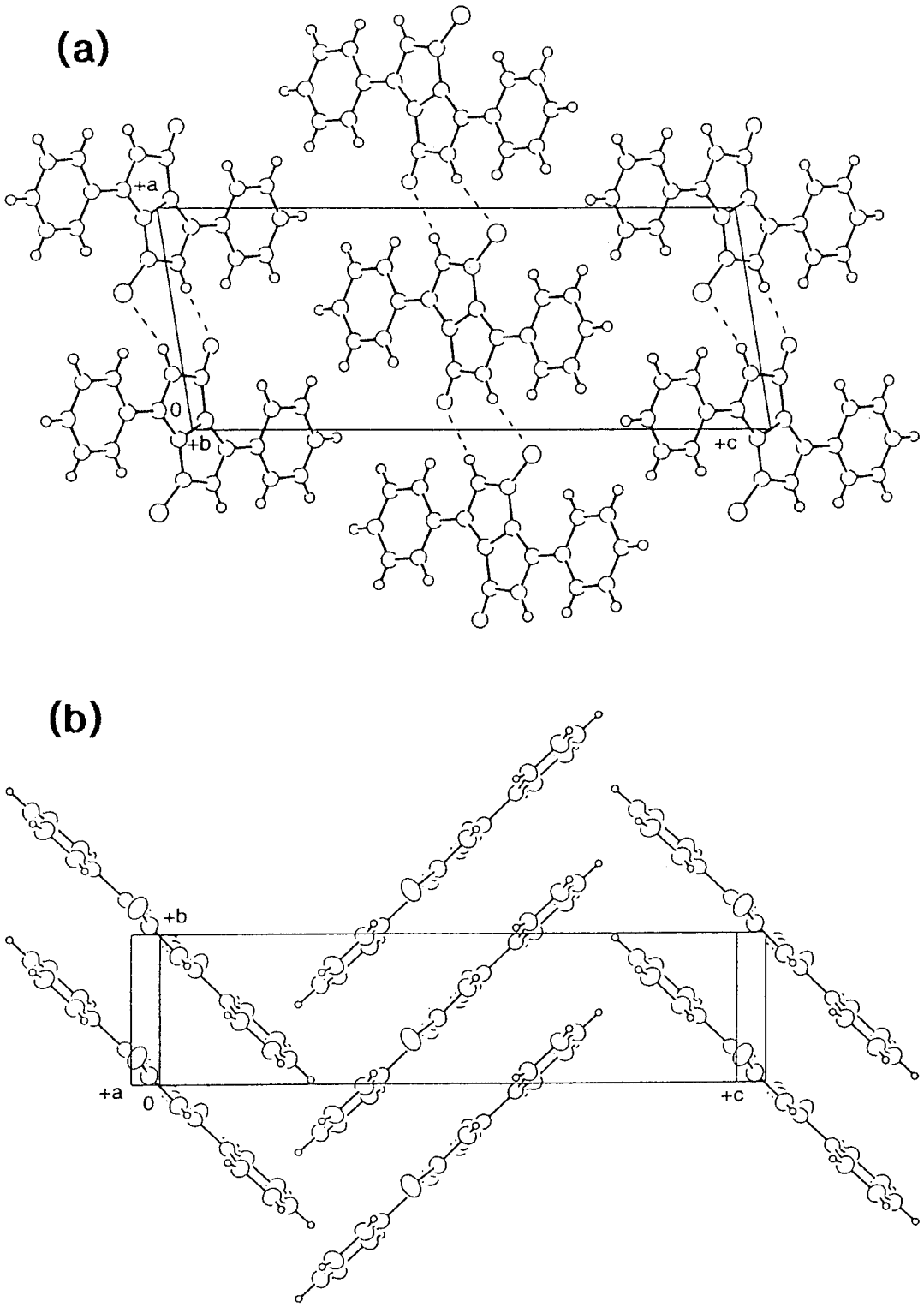

Figure 2. Projection of the crystal structure of MTPP: (a) onto the (*a*,*c*) plane, and (b) onto the (*b*,*c*) plane.

to that of the conventional blue filter based on copperphthalocyanine, or even exceeds its performance.

The temperature dependence of absorption spectra before and after vapor treatment were measured in the temperature range between 20 and 300 K and is shown in Figures 7a and 7b, respectively. No appreciable spectral changes were observed in the absorption spectra before vapor treatment. On the other hand, the absorption spectra after vapor treatment exhibit a remarkable temperature dependence around the longest-wavelength band at 700 nm. This indicates that the present band is quite structure-sensitive, namely sensitive to lattice contraction at low temperatures and is due to intermolecular interactions.

A similar temperature dependence is also observed only in modification III of DTPP.[19]

3.4. X-ray Diffraction Diagrams. Figure 8 shows the X-ray diffraction diagrams before and after vapor treatment. The broad band around 26° is due to the glass substrate used. The phase before vapor treatment is characterized by a single diffraction peak around 6.5°. Vapor treatment then induces crystallization as shown by the diffraction peaks around 6.5, 13, 19, and 26°.

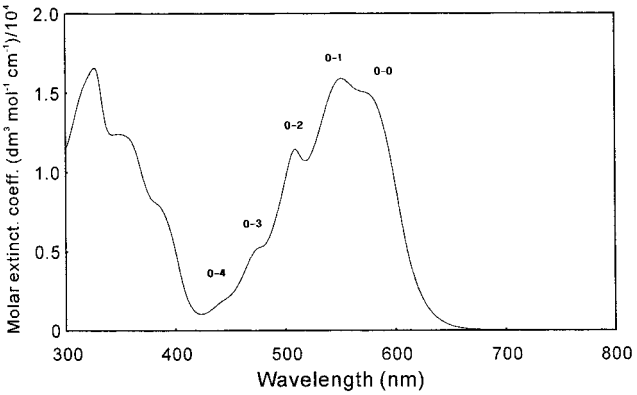

Figure 3. Solution spectrum of MTPP in DMSO.

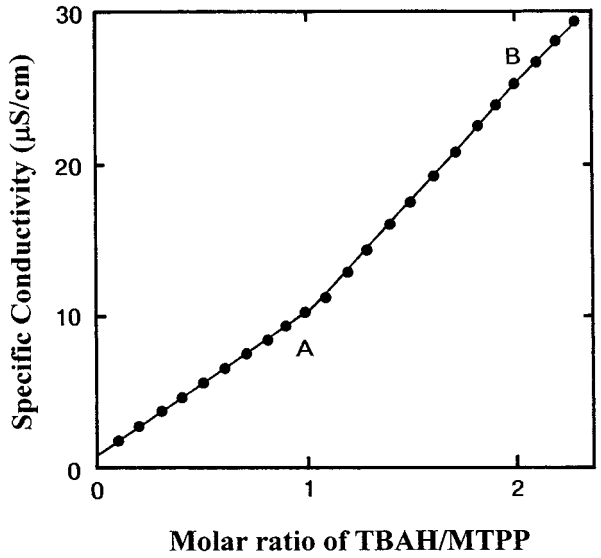

Figure 4. Conductometric titration of MTPP in DMSO by means of TBAH.

The diffraction peak around 26° corresponds to the diffraction along the stacking axis. This indicates that the molecules are ordered along the stacking axis due to vapor treatment. Because of the present ordering of the molecules, the absorption band is displaced from 610 to 700 nm (Figure 6) and exhibits an appreciable temperature dependence (Figure 7b). Then, we tried to assign the observed diffraction peaks on the basis of the analyzed crystal structure. However, the assignment was unsuccessful. Particularly, the diffraction peak around 6.5° was not assignable. This indicates that the phase of evaporated, vapor-treated MTPP is different from the crystalline phase determined by the X-ray structure analysis.

3.5. IR Spectra in Evaporated Films. The IR-spectra before and after vapor treatment are shown in Figure 9. The broad band around 3000 cm^{-1} is assigned to the hydrogen-bonded NH-stretching band. The C═O and C═S bands appear around 1650 and 1200 cm^{-1}, respectively. The present result reveals that the intermolecular NH···O hydrogen bonds are formed in evaporated films. Vapor treatment displaces both the NH and C═O stretching bands toward lower wavenumbers by about 44 and 12 cm^{-1}, respectively, showing the stabilization of the hydrogen bond. This indicates that the molecules are, to some extent, rearranged so as to reinforce the intermolecular NH···O hydrogen bond.

Due to the formation of hydrogen bond, the NH stretching band is considerably displaced to ca. 3100 cm^{-1} relative to the free NH stretching band (usually around 3500 cm^{-1}). So the

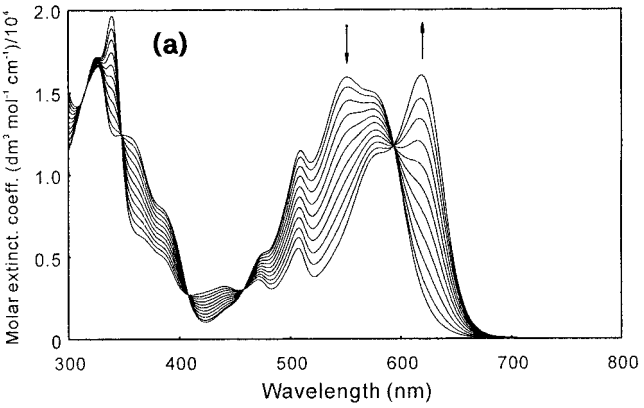

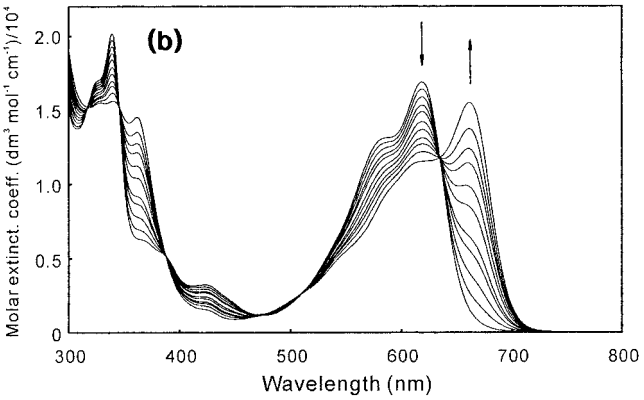

Figure 5. Solution spectra of MTPP on deprotonation: (a) from the initial point to point A, and (b) between points A and B.

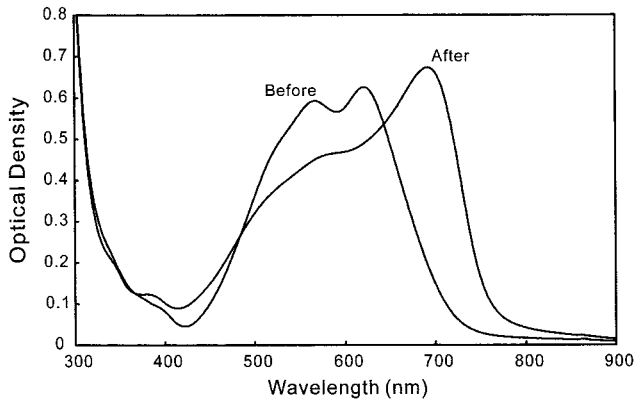

Figure 6. Absorption spectra of evaporated MTPP before and after vapor treatment.

extent of the present stabilization energy can serve as a measure of the strength of the intermolecular hydrogen bond as evaluated for DPP[7] and DTPP.[19] Judging also from the N/O and N/S distances in DPP, MTPP, and DTPP as presented in section 3.1, the hydrogen bond in DPP (NH···O) is the strongest and becomes weaker in the order of DTPP (NH···S) and MTPP (NH···S and NH···O).

3.6. Thermogravimetric Analysis (TGA) of Powdered MTPP. Figure 10 shows the weight loss of powdered DPP, MTPP, and DTPP under vacuum or in air as a function of temperature. Under vacuum, the weight loss of MTPP and DTPP behaves in a similar way while DPP persists at higher temperatures. In air, DPP is again quite stable even at 400 °C while MTPP and DTPP start to sublimate or decompose at about 292 and 335 °C, respectively.

The intermolecular forces which hold molecules together in the solid state are closely correlated with sublimation temper-

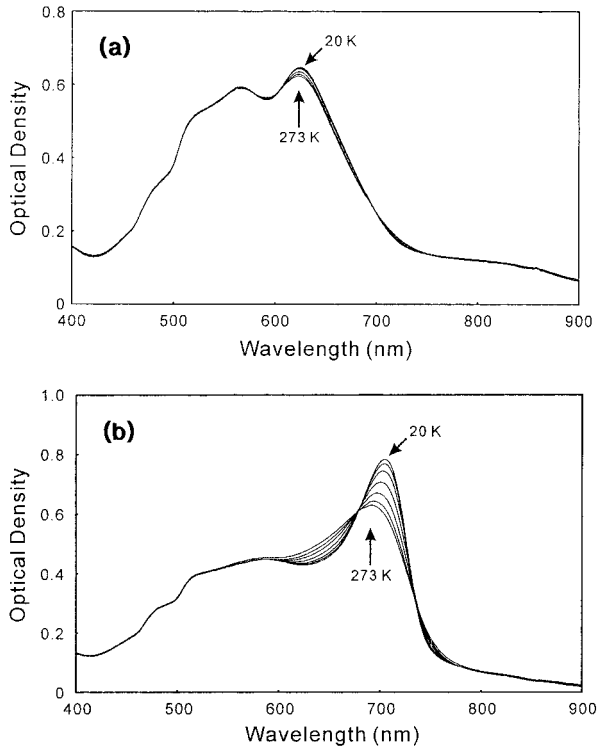

Figure 7. Temperature dependence of absorption spectra: (a) before vapor treatment, and (b) after vapor treatment.

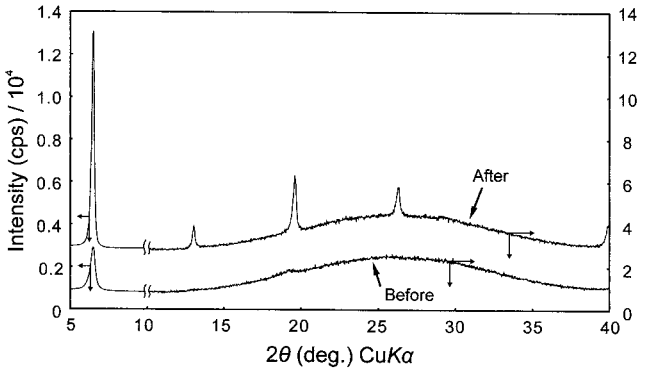

Figure 8. X-ray diffraction diagrams of evaporated MTPP before and after vapor treatment.

ature as well as solubility in solvents. The present TGA results are fully consistent with the hydrogen-bond strength as evaluated by IR and X-ray analyses. Furthermore, DPP is quite insoluble in any solvents while DTPP is more soluble than DPP and MTPP is much more soluble.

3.7. Polarized Reflection Spectra and the Direction of the Transition Dipole. Figure 11 shows the polarized reflection spectra of MTPP single crystals measured on the (001) plane by means of a microscope-spectrophotometer. Prominent reflection bands appear around 550 and 620 nm for polarization parallel to the *a*-axis, i.e., the direction of the intermolecular hydrogen bond. On the contrary, polarization perpendicular to the *a*-axis, i.e., along the stacking axis, quenches these visible bands. Instead, a small reflection band is observed around 640 nm. The fact that the two visible bands (550 and 620 nm) appear and disappear simultaneously by polarized light indicates that the two bands belong to the same electronic transition and the longest-wavelength band is attributed to the 0−0 transition, and the second longest-wavelength broad band might include the 0−1 and 0−2 transitions.

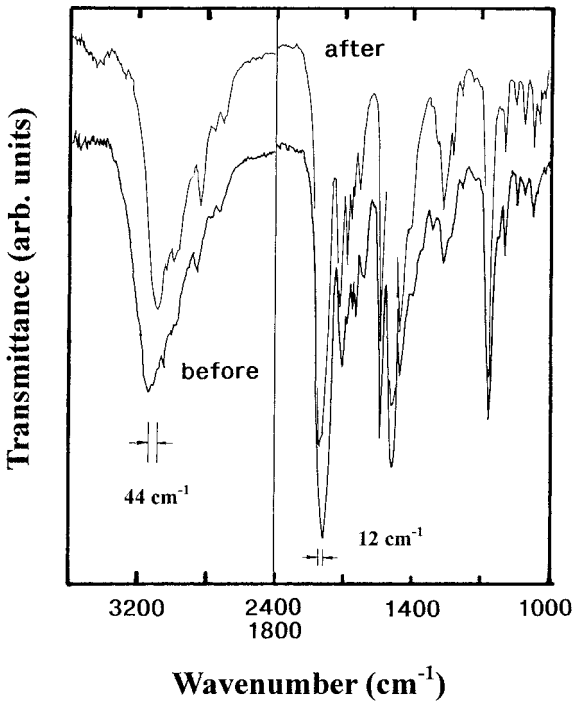

Figure 9. IR absorption spectra of evaporated MTPP before and after vapor treatment.

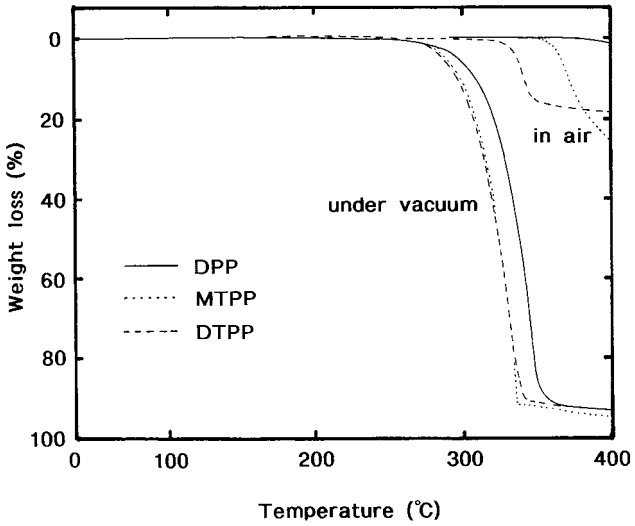

Figure 10. TGA measurements of powdered DPP, MTPP, and DTPP under vacuum and in air.

As apparent from the polarized reflection spectra (Figure 11), the transition moment of MTPP points the direction of the intermolecular hydrogen bonds based on NH···O and NH···S. On the one side, the intermolecular hydrogen bonds hold MTPP molecules together to stabilize the system and also to suppress the solubility in solvents. On the other hand, the hydrogen bonds align the transition dipoles in a fashion "head-to-tail" and thus displace greatly the absorption band toward longer wavelengths. This is the effect caused by interactions between transition dipoles ("exciton coupling effect"). The spectral displacements due to exciton coupling in DPP derivatives and DTPP are fully discussed in our previous reports.[11,20]

The small band around 640 nm in Figure 11 can be ascribed to an intermolecular charge transfer (CT) band along the stacking axis. This sort of CT transition is often observed in sulfur-containing compounds, in which the molecules are stacked in

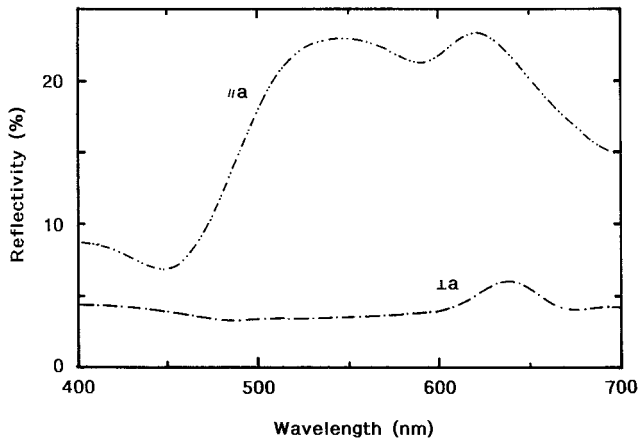

Figure 11. Polarized reflection spectra measured on the (001) plane of MTPP single crystals.

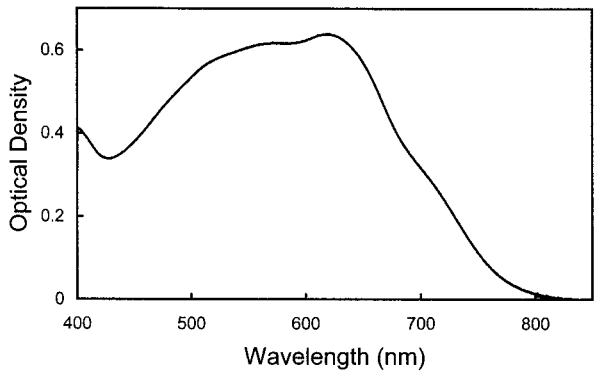

Figure 12. Diffuse reflectance spectrum of MTPP as synthesized.

a herringbone fashion. In fact, a similar CT band is also observed in modifications I and II of DTPP.[19]

3.8. Diffuse Reflectance Spectrum of Powdered MTPP. Figure 12 shows the diffuse reflectance spectrum of powdered MTPP as synthesized. The powdered phase is identified as the same phase of the analyzed structure. Therefore, the diffuse reflectance spectrum of powdered MTPP resembles the polarized reflection spectra of MTPP measured on single crystals (Figure 11). The 0−0, 0−1 and 0−2 transitions are clearly recognized. In addition, an absorption shoulder around 700 nm is also recognized which is an indication of the second phase of MTPP as shown in the Figure 8 of the vapor-treated phase. This means that a small portion of the second phase is mixed in MTPP powders as synthesized.

3.9. Similarities between MTPP and DTPP. As we have seen, the crystal structure of MTPP is isomorphous with modification I of DTPP and the molecules are arranged in a "herringbone" fashion (Table 1). Modifications I and II of DTPP are quite similar. On the other hand, modification III of DTPP crystallizes in a fashion "bricks in a brick wall". Because of this structure, modification III exhibits an intense near-IR absorption (850 nm); i.e., a large bathochromic shift from 700 to 850 nm. A similar spectral shift is also observed in MTPP from 620 to 700 nm (Figure 6), and both absorption bands exhibit remarkable temperature-dependence (Figure 7b). In contrast, the CT band along stacking axis is only observed in MTPP (Figure 11) and DTPP I and II,[19] in which all molecules are stacked in a "herringbone" fashion. These observations suggest that the second phase of MTPP is quite similar to modification III of DTPP.

4. Summary

The electronic structure of MTPP has been studied on the basis of the crystal structure and intermolecular interactions. The present investigation can be summarized as follows:

1. The crystal structure of MTPP is isomorphous with modification I of DTPP. Therefore, MTPP behaves spectroscopically as DTPP rather than DPP.

2. The polymorphic properties of DTPP are also observed in MTPP.

3. The absorption spectrum of evaporated MTPP suggests a potential application for LCD blue filters.

References and Notes

(1) Iqbal, A.; Cassar, L.; Rochat, A. C.; Pfenninger, J.; Wallquist, O. *J. Coat. Technol.* **1988**, *60*, 37.
(2) Mizuguchi, J.; Grubenmann, A.; Wooden, G.; Rihs, G. *Acta Crystallogr.* **1992**, *B48*, 696.
(3) Mizuguchi, J.; Grubenmann, A.; Rihs, G. *Acta Crystallogr.* **1993**, *B49*, 1056.
(4) Mizuguchi, J. *Acta Crystallogr.* **1998**, *C54*, 1482.
(5) Mizuguchi, J.; Matumoto, S. *Z. Krisallogrt.-NCS* **2000**, *215*, 195.
(6) Mizuguchi, J.; Wooden, G. *Ber. Bunsen-Ges. Phys. Chem.* **1991**, *95*, 1264.
(7) Mizuguchi, J.; Rihs, G. *Ber. Bunsen-Ges. Phys. Chem.* **1992**, *96*, 597.
(8) Mizuguchi, J. *Ber. Bunsen-Ges. Phys. Chem.* **1993**, *97*, 693.
(9) Mizuguchi, J.; Rochat, A. C. *Ber. Bunsen-Ges. Phys. Chem.* **1992**, *96*, 708.
(10) Mizuguchi, J. *Ber. Bunsen-Ges. Phys. Chem.* **1993**, *97*, 684.
(11) Mizuguchi, J. *J. Phys. Chem. A* **2000**, *104*, 1817.
(12) Mizuguchi, J.; Rochat, A. C. *J. Imag. Sci.* **1988**, *32*, 135.
(13) Mizuguchi, J.; Homma, S. *J. Appl. Phys.* **1989**, *66*, 3104.
(14) Mizuguchi, J. *J. Appl. Phys.* **1989**, *66*, 3111.
(15) Mizuguchi, J.; Rochat, A. C. *J. Imag. Technol.* **1991**, *17*, 123.
(16) Mizuguchi, J.; Giller, G.; Baeriswyl, E. *J. Appl. Phys.* **1994**, *75*, 514.
(17) Mizuguchi, J.; Rochat, A. C.; Rihs, G. *Acta Crystallogr.* **1990**, *C46*, 1899.
(18) Mizuguchi, J.; Arita, M.; Rihs, G. *Acta Crystallogr.* **1991**, *C47*, 1952.
(19) Mizuguchi, J.; Rochat, A. C.; Rihs, G. *Ber. Bunsen-Ges. Phys. Chem.* **1992**, *96*, 607.
(20) Mizuguchi, J. *Electrophotography* **1998**, *37*, 58.
(21) Mizuguchi, J. *Electrophotography* **1998**, *37*. 67.
(22) Rochat, A. C.; Iqbal, A.; Wallquist, O. U.S. Patent 5,017,706, 1989.
(23) Mizuguchi, J. *Krist. Tech.* **1981**, *16*, 695.
(24) Mizuguchi, J. *Z. Kristallogr.* **1999**, *214*, 677.
(25) Stewart, J. J. P. *MOPAC93* Fujitsu.
(26) Kogo, Y.; Kikuchi, H.; Matsuoka, M.; Kitao, T. *JSDC* **1980**, *96*, 475.
(27) Takata, S.; Ono, Y.; Ueda, Y. *Chem. Pharm. Bull.* **1985**, *33*, 3077.
(28) Mataga, N.; Nishimoto, K. *Z. Phys. Chem. Neue Folge* **1957**, *13*, 140.